

# Design of the Electromagnetic Particle Injector (EPI) for Tokamak Deployment

R. Raman, Member, *IEEE*, R. Lunsford, J.A. Rogers, A. Brooks, A. Maan, L. Perkins

**Abstract**— Both predicting and controlling disruptions are critical and urgent issues for ITER as some disruptions with a short warning time may be unavoidable. For these cases, a rapid response disruption mitigation system referred to as the Electromagnetic Particle Injector (EPI) is being developed. The primary advantages of the EPI are its fast response time and high velocity, which have been demonstrated in offline experiments [R. Raman et al., *Nucl. Fusion* 61 (2021) 126034]. The EPI is capable of accelerating a metallic sabot electromagnetically using a rail gun to the required velocities ( $> 2$  km/s) within 2 ms. Two high-field racetrack magnets, able to generate fields over 2 T are positioned above and below the rails to permit high velocity at low rail currents, a requirement to minimize electrode erosion. At the end of the acceleration phase, a sabot capture mechanism retains the spent sabot inside the vacuum chamber that houses the EPI. At this point, it releases well-defined microspheres, or a shell pellet, of a radiative payload into the disrupting plasma. A remotely operated sabot loading system positioned behind the injector contains several pre-equipped sabots that can be loaded by an operator from the tokamak control room. The injector is interfaced to the tokamak through a guide tube attached to the front of the EPI vacuum chamber. The advantages of the EPI system over other disruption mitigation systems under consideration are described in conjunction with the details of an EPI system designed for near-term test on an existing large tokamak.

**Index Terms**— EPI, SPI, DMS, thermal quench, disruption

## I. INTRODUCTION

The tokamak is the most rigorously researched fusion energy concept to-date, and technologically closest to net electrical power generation. Confining a reactor sized tokamak plasma requires that toroidal plasma currents in the 10 to  $>20$  MA range be driven within the plasma to generate most of the confining poloidal magnetic fields [1]. As the tokamak plasma relies on a large magnitude of internally driven plasma current, there exists the possibility that magneto hydro dynamic (MHD) instabilities within the plasma, or other external factors such as eroded parts of the vacuum vessel components falling into the plasma discharge, could initiate a major plasma disruption. Once a major disruption is underway, it becomes essential that measures be rapidly implemented to ensure that the resulting stored energy within the plasma is quenched in a manner so as not to damage the vacuum vessel

components. The stored plasma energy in the ITER plasma is 350 MJ, which is much higher than the  $<10$  MJ available for disruption mitigation studies in present tokamaks.

All tokamak-based reactors will thus need to rely on one or more disruption mitigation systems (DMS). The DMS is the final line of defense for protecting the costly tokamak infrastructure. The DMS injects a radiative payload into the target plasma which, under an ideal scenario, would uniformly radiate most of the plasma energy to the vessel walls on a short time scale known as the thermal quench (TQ) and also suppress the formation of runaway electrons [2, 3, 4]. The TQ time scale on ITER is estimated to be about 3 ms [5]. But recent JOREK and INDEX simulations of ITER SPI predict that ITER plasmas may have TQ durations up to 10 ms [6, 7] due to size effects. The Shattered Pellet Injection (SPI) system has been chosen as the primary DMS for ITER [8]. The SPI injects frozen cryogenic pellets comprised of gases such as Neon, Argon, Deuterium, Hydrogen, or combinations of these into the disrupting plasma. Prior to reaching the plasma, the frozen pellet is shattered by impact on a target plate so that many smaller fragments are simultaneously injected. Off-line experiments have shown that during the fragmentation process, depending on the injection velocity, a significant portion of the injected fragments can vaporize [9]. As a result, the injected material consists of a leading edge of vaporized gas followed by frozen fragments of various shapes, sizes and velocity. Due to the stochastic nature of the shattering process, the fragment arrival time at the plasma edge is not a precise number. For instance, on DIII-D, 200 m/s pellet injection velocities result in the fragments which are spread out over a 20 ms interval, with some fragments continuing to arrive even after the thermal quench is over [10]. The SPI system on DIII-D has an overall response time, from trigger time to initial plasma impact of 25 ms [10]. The estimated SPI injection velocities for ITER are about 200 – 400 ms/s and as such the response times may be similar for ITER. At this velocity it would take 5 to 10 ms for the fragments to transit the plasma minor cross section, which is much longer than the 3 ms TQ lower time limit.

Because the ITER plasma is so much larger, and energetic than present experiments, reliable MHD modeling is the only way to confidently extrapolate to ITER. However, given the complex nature of the SPI injection parameters, MHD modeling of the resulting plasma behavior has been challenging. As of

Paper submitted on 20 August 2023 “This work was supported in part by the U.S. Department of Energy under Grants DE-SC0006757, DE-AC02-09CH11466 and PPPL sub-contract S017736. (Corresponding author: R. Raman)

R. Raman and J.A. Rogers are with the University of Washington, Seattle, WA, 98195 USA (Email: raman@aa.washington.edu).

R. Lunsford, A. Brooks, A. Maan, and L. Perkins are with the Princeton Plasma Physics Laboratory, Princeton, NJ (Email: rlunsfor@pppl.gov). Color versions of one or more of the figures in this article are available online at <http://ieeexplore.ieee.org>.

now MHD simulations at present do not consider the pre-SPI gas load [11, 12], which can be quite significant at high injection velocities. This pre-SPI gas load could initiate a TQ well before the bulk of the SPI fragments penetrate sufficiently far into the plasma. As a result, the capability of the SPI system for protecting ITER infrastructure may not be known until ITER begins operations.

Another important factor is the nature of the plasma radiative collapse itself. An outside-to-inside thermal collapse occurs when the outer regions of the plasma are initially cooled. After adequate radiative material assimilation by the plasma [13], MHD instabilities are relied upon to transport the radiative material to the plasma core which can lead to uncertainty in the seeding time. A preferred methodology would be an inside-to-outside thermal quench where the radiative material is directly deposited within the plasma core, thus avoiding the reliance on plasma transport. By depositing the radiative material directly in the plasma core (where the runaway current channel originates), and by controlling the amount of injected material so as not to cool the core plasma to very low temperatures, it should be easier to suppress the formation of the runaway current channel. As the minor radius of the ITER plasma is 2 m, velocities on the order of about 1 km/s (preferably higher) are needed to permit the radiative material to penetrate deep into the core plasma before a TQ is over. To address these needs new injection methods that permit both higher injection speed and faster overall response time are essential and need to be tested on present tokamaks.

During a recent review of the US Fusion program needs it was concluded that, given the cost and complexity of the ITER device, and the persisting DMS unknowns, alternate back-up systems, capable of improved payload injection capability should be developed and tested on present tokamaks. The Electromagnetic Particle Injector (EPI) has the potential to be just such an alternative. The remainder of this paper is organized as follows. Section II describes the EPI, section III describes the EPI design for a near-term tokamak test, and section IV is a brief conclusion of the main results from this paper.

## II. THE ELECTROMAGNETIC PARTICLE INJECTOR (EPI)

The EPI system is based on the Rail Gun concept. It accelerates a metallic aluminum sabot, with the contact edges coated with tungsten, to high velocity with an electromagnetic impeller and releases any radiative payload that would fit into the sabot, or a shell pellet.

A bent metallic plate termed a sabot is placed under spring tension between two conducting rails separated by about 2-3 cm as shown in Figure 1a. Figure 1b shows the electrical schematic. The payload consisting of granules of a known size and distribution, or a thin wall shell pellet containing the payload, is placed inside the hollow chamber of the sabot. A capacitor bank is connected to one end of the rails. Discharging the capacitor bank causes the current to flow along the rails through the sabot and the  $\mathbf{J} \times \mathbf{B}$  forces resulting from the interaction between the magnetic field created in the region between the rails and the current through the sabot accelerates the sabot and the payload.

At the end of its acceleration, within 2 ms, the sabot is captured, and the payload is released. For the EPI, as described in Reference [14], the use of high-field external boost coils (located above and below the rails) can increase the magnetic field to very high levels ( $>24$  T should be possible in the future) thereby reducing the current through the rails to very low levels. The low mass sabot needed for rapid acceleration of the EPI payload necessitates the use of an external boost field to reduce the sabot currents to mechanically tolerable levels. This allows the velocities over 1 km/s required for ITER core penetration [15].

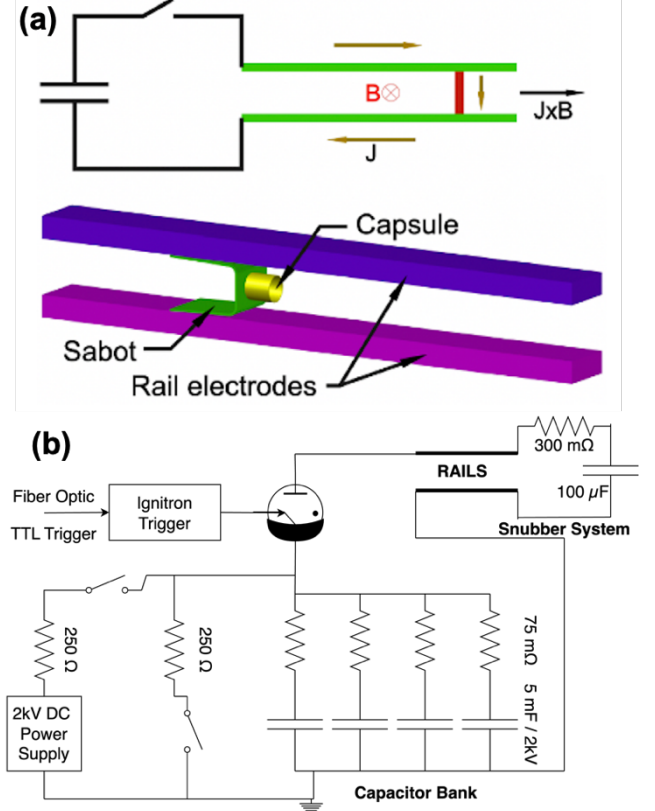


**Fig. 1.** (a) The EPI consists of two rails with a metallic sabot placed between the rails. Driving current from one rail to the next through the metallic sabot generates a  $\mathbf{J} \times \mathbf{B}$  force that propels the sabot. Adding external coils to increase the magnetic field between the rails reduces the required rail current to achieve a given acceleration force. Reproduced courtesy of IAEA. Figure from [16]. Copyright (2019) IAEA. (b) Simplified drawing of the 20 mF EPI electrical circuit including the passive snubber protection system.

In high-field tokamaks it may be possible to mount a compact EPI system inside the outer leg of the toroidal field coil to take advantage of the intrinsic high magnetic fields. This has the added advantage that the overall response time from trigger time to the material being deposited deep inside the tokamak plasma could be reduced to about 3 ms [14]. Unlike in some systems such as a gas gun in which the maximum acceleration force occurs at the start of the acceleration process, the current rise time controlling the acceleration in the EPI can be tailored either using a suitably sized capacitor bank or using a pulse forming network, ensuring that the maximum acceleration force does not appear

until the pellet has gained some velocity. This would reduce the stress on the protective shell allowing more flexibility in the design of the shell pellet.

References [14-16] discuss in detail the requirements of the EPI system for ITER. A near-term test on multiple tokamaks, combined with MHD modeling, is needed to establish the payload size and composition requirements for injection into ITER discharges. The first test of the EPI for disruption mitigation applications relied on simple meter long brass rails with a simple boots coil that generated 0.3 T external fields [16]. Using a 3.2 g sabot and a 40 kJ capacitor bank operated at 2 kV with 50 kA of rail current this system was able to demonstrate a sabot velocity of 150 m/s (pre-payload release) within 1 ms, consistent with calculations. This motivated the design and operation of a system in a configuration that could be deployed on a tokamak. This system was much more compact with rails less than 50 cm long, but with the external coil boost field increased to 3 T. Using a 4.1 g sabot and a 10 kJ capacitor bank operated at 1 kV, and with 25 kA of rail current this system [14] was able to demonstrate a velocity of 200 m/s within 1 ms, also consistent with expectations. This system also demonstrated the capability to capture the spent sabot. Calculations for an ITER-class system indicate that velocities of over 2 km/s should be achievable using external boost magnetic fields of about 24 T [14].

Ref. [14] describes experimental results from the second generation of the EPI device that used 3 T boost magnetic fields. It compares the improved parameters from EPI-2 to that obtained in the first-generation EPI-1 device that used 0.3 T boost magnetic field to show that the improved performance is consistent with the calculated projections. It then describes the significant performance improvements that can be realized when extremely high levels of boost magnetic field could be used in a reactor-class injector, made possible using high temperature superconducting coils. However, a next step tokamak system, because of cost constraints, would most likely use normal conducting magnetic field coils. It also describes in detail the open issues for the deployment of EPI in a reactor. This paper differs from Ref. [14] in that it presents the actual hardware design to be used for a next step tokamak deployment, with a focus of how to remotely load the cartridges, and the details of the vacuum chamber. It describes the actual systems that is at present being assembled at PPPL to prepare it for an eventual tokamak deployment.

### III. EPI CONFIGURATION FOR A NEAR-TERM TOKAMAK TEST

The EPI system for a near-term tokamak test would be designed for a nominal injection velocity of 400 m/s, with the capability for a maximum velocity of 1000 m/s, as described in Fig. 8 of Reference [14]. The EPI-2 system is currently being re-assembled at PPPL to prepare it for tokamak deployment. The total injected mass would be about 3.9 g of which the payload mass would be up to 0.5 g. For comparison, as part of the DMS studies on DIII-D, a radiative mass of 0.4 g Ne is typically injected in high powered super shots [2,10]. As the EPI payload is anticipated to penetrate deep into the target plasma, and so be more fully assimilated by the target plasma,

an injection mass of <0.4 g should be adequate to attain full thermal quench on present experiments. WEST, DIII-D, SPARC, KSTAR, EAST, ASDEX-U, and ST-40 are all suitable candidates for such a test. Indeed, present experiments on DIII-D that used the Shell pellet were able to achieve rapid shutdown with only 21 mg of boron power [17]. Part of the reason for the 500 mg payload specification is to connect with present SPI injection parameters.

Driving a payload to 400 m/s over 2 ms is an explosive process which results in wear on the conducting rails. However, utilization of the 3 T boost fields has been shown to reduce the necessary current to a level where present off-line experiments have shown that the electrode erosion is sufficiently small with molybdenum rail electrodes to permit about 40 injection pulses before the electrodes need to be re-surfaced. For tokamak deployment, tungsten electrodes are being considered, as they should perform better, permitting a higher number of injections before electrode re-surfacing. Although tungsten was the preferred choice for this reason, Molybdenum was initially used due to budgetary constraints. Eroded material entering the tokamak may not be an issue as discussed in Section 5.1.3 in Ref. [14]. The capability of tungsten electrodes will be tested in the off-line experiments at PPPL. Calculations show that by operating at higher rail currents, closer to the values used on EPI-1, 1 km/s velocities would be possible. At 3 T boost fields this would lead to increased electrode erosion, so that the number of such injection pulses would be reduced, and they would be limited to specific previously well documented cases at 0.4 km/s to assess any additional benefits of this increased velocity injection on the DIII-D/WEST-scale tokamaks. The field from a magnetic dipole falls off very rapidly as the inverse third power of the distance from the coil. The effective radius of the racetrack coil is 4 cm and the coil may be located about 2 m from the tokamak, which should reduce any stray fields at the tokamak vicinity to below a Gauss. In addition, this field would only be energized during the operation of the EPI system so that it should not interfere with normal tokamak operation.

The materials that could be injected in ITER include B, BN, and W. These or combinations of these, and the payload delivery method, i.e., whether they are individual spheres, or encased within a shell pellet, needs experimental tokamak injection studies in combination with MHD simulations to assess the resulting response of the tokamak plasma. Near term tokamak experiments could also use C or other suitable materials for the studies.

Figure 2 shows the overall layout of the EPI-2 system for a tokamak test with a top-down view of the main components shown in Fig. 3. To the right of the core EPI system is the sabot capture system. To the left of the core EPI system is the remotely operated sabot loading system. Attached to the bottom of the vacuum chamber is the vacuum pumping system where the isolation gate valve and the turbo pump are shown. These individual systems will now be described in more detail.

In front of the sabot capture system is a vertical cylinder hanging down from the vacuum tank. This chamber is for collecting and retaining the spent sabots. The vacuum chamber that encases the EPI system would retain the spent sabots. On a periodic basis after numerous spent sabots have accumulated, these would be removed during routine maintenance of the

injector. The payload released by the sabot will travel along a guide tube that interfaces the EPI vacuum chamber to the tokamak vessel. It would be directed at some tangency to the plasma discharge so that in the absence of plasma, the payload material could impact a metallic tungsten armor plate that is positioned on the opposite wall along the injection direction or exit the tokamak vessel through a port at this location.

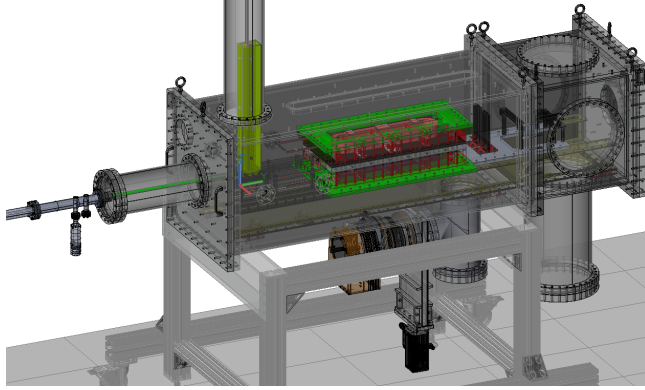


**Fig. 2.** 3D drawing of the EPI system showing the vacuum chamber inside which are the core EPI system, the sabot capture system and the remote sabot loading system. The core EPI system can be identified by the green plates.

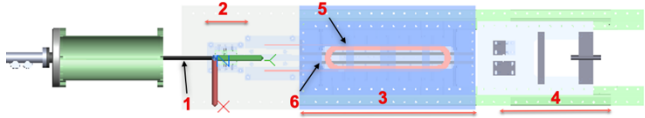


**Fig. 3.** Top-down view of the main components inside the vacuum tank. Moving from the left to the right are seen (1) the precise sabot insertion tool, (2) the sabot cartridge area (3) the core EPI region and (4) finally the sabot capture system. Also shown are (5) the EPI coils and (6) the EPI rails.

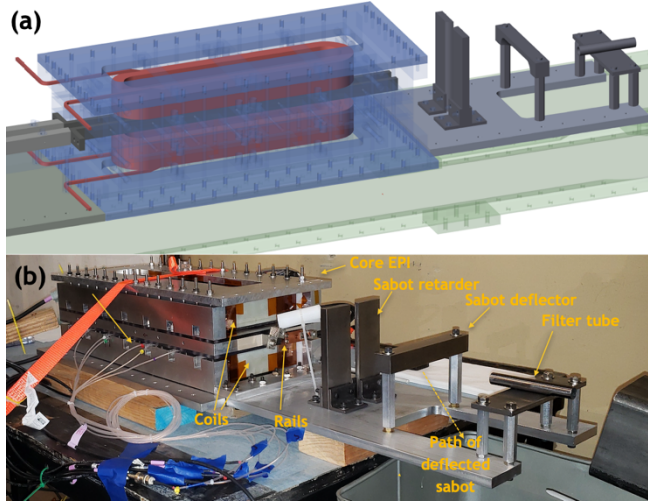


**Fig. 4.** Shown are (a) drawing of the main components within the core EPI hardware and the sabot capture system details, (b) photo showing the core EPI hardware and the sabot capture

system during off-line testing. Reproduced courtesy of IAEA. Figure from [14] Copyright (2021) IAEA.

Figure 4(a) shows the main internal components inside the core EPI hardware. It consists of the rails, shown in grey color and fabricated out of molybdenum. Prior to a tokamak deployment, tungsten rails would be tested as tungsten rails are expected to erode less. Above and below the rails are mounted racetrack shaped magnetic coils shown in red color. Structural support is provided on either side of the racetrack coils. The structural supports can be seen in Fig. 2 of Ref. [15]. A detailed ANSYS simulation was carried out that indicated that these coils and the support structure can be operated at fields up to 3 T. The details of this calculation and the support structure details are shown in Fig. 3 of Ref. [15]. A photo of the fully assembled core EPI hardware can be seen Fig. 4 (b).

Seen at the front of the core EPI hardware is the sabot capture assembly. The first component is the sabot retarder system. This is composed of edge rounded metal plates with the spacing between them calibrated to be slightly less than the maximum width of the metallic sabot that would pass through it. As a result, as the sabot passes through the gap in the plates, friction between the sabot and the plates causes the sabot to slow down. This causes the payload inside the sabot cavity, which is still traveling at its original velocity, to separate from the sabot. The sabot then encounters the tungsten sabot deflector plate which contacts the top 1 mm of the sabot edge, causing the sabot to be deflected at a downward angle. A catch tank located at an appropriate distance in front of this deflector plate collects and retains the spent sabot. The payload itself then travels unimpeded through a small diameter filter tube, the purpose of which is to permit only material entering this small diameter tube from progressing into the tokamak vacuum vessel. Thus, any fragments resulting from the sabot deflection process, that generally would not have a linear trajectory, would not be able to pass through this filter tube. The sabot deflection concept was tested on a 2 km/s two stage gas gun that was deployed on the SSPX spheromak at the Lawrence Livermore National Laboratory [18].

Shown in Fig. 5 are the details of the remote sabot loading system. The first component is a vertical rectangular chamber inside which several pre-loaded sabots are stacked. It is also referred to as the cartridge chamber. The height of this chamber could be adjusted to increase the number of stored sabots. In the inset is shown a top-down view of the components inside the rectangular cartridge chamber. Long bars (indicated by the number 1) covering the entire height of the cartridge chamber are present on either side of the sabot. These are shaped in a manner so that a sabot that is dropped into this chamber would naturally align correctly and sit on top of the sabot below it. To more precisely align the sabots, a vertical wedge-shaped region that loosely conforms to the inner dimensions of the sabot is bolted to the back end of the cartridge chamber. This is indicated by the number 2 in Fig. 5. The combination of both the outer and the inner sections of the sabot guide rails leave a small gap that conforms to the shape of the sabot, permitting the stacked sabots to be well aligned. On the top of the last sabot would be placed a loading section (of a specified weight to be experimentally determined) attached to two cylindrical posts.

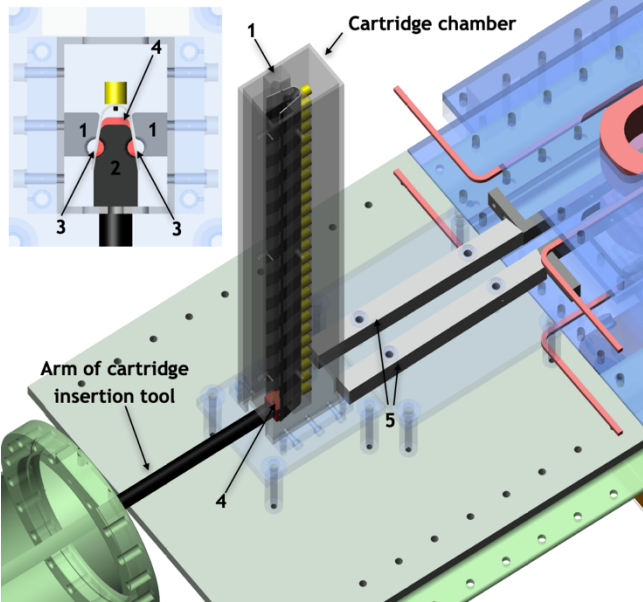


**Fig. 5.** 3D view of the sabot loading system showing several sabots stacked on top of each other. The black cylindrical rod is a precise sabot insertion tool. The inset shown is a top-down view of the rectangular sabot cartridge area.

The location of the cylindrical posts is marked by the number 3 in Fig. 5. The cylindrical rods pushing on the top of the sabot would make it easier for a new sabot to drop into place after a sabot is inserted into the EPI core. This small added weight is to overcome any small friction between the sabots and the surrounding alignment structures that may cause some sabots to stick in place and not drop down on their own. An active mechanical pusher arrangement could also be employed but is believed to be unnecessary at this time.

In order for the payload microspheres to remain robustly inside the sabot cavity, they either need to be contained inside a thin elongated cylindrical shell capsule composed of B or BN or the microspheres need to be weakly bonded to each other so that they do not dribble out of the sabot cavity. Thus, it is not necessary for the thin shell to be strong enough to withstand the acceleration forces. If a spherical shell pellet is used, it may need to be designed with a short flat region around the circumference that makes contact with the sabot chamber, or the entire injector may need to be inclined up at a small angle to force the payload to move towards the back of the sabot chamber. This second approach is being adopted for the present system.

At the bottom of the sabot loading system is the sabot insertion system. This is a linear horizontal tool (part number: Actuator-SLO, RPL-75-20\_MS-W4, Thermionics, Northwest, inc.) that allows the sabot to be precisely located inside the core EPI system. Attached to the front end of this tool is a wedge-shaped section (indicated by the number 4 in Fig. 5) that loosely fits inside the sabot inner cavity. The sabot insertion tool can be programmed for a specified insertion depth. When activated it would insert the lowermost sabot to the specified location and then withdraw to its resting location. This would cause a new sabot to fall into place. As the sabot is being inserted, it

traverses ceramic guide rails (indicated by the number 5 in Fig. 5) that separate the metallic rail electrodes from the sabot cartridge assembly. The sabot insertion position is not a single location. It can be varied from shot to shot remotely through the computer control interface that would operate this system.

TABLE I  
COMPARISON OF THE POTENTIAL CAPABILITIES OF EPI WITH  
THOSE OF THE SPI INJECTION CONCEPT

SPI	EPI
There is a pre-gas load before SPI fragments enter plasma	No gases used. Pre-gas load need not be modelled in MHD simulations
Stochastic payload fragment size, shape and velocity distribution makes MHD modeling more difficult	Well defined payload size, shape and velocity should result in easing MHD modeling resulting in more reliable extrapolation to reactors
Payload injection velocity limited to $\sim 200$ -500 m/s	Velocity greater than 2 km/s is possible
Pre-gas load amount increases with SPI injection velocity	NA
Reliance on unpredictable MHD to transport radiative material to the core	Potential for depositing needed radiative payload in the core avoids reliance on unpredictable MHD processes
Insufficient time for payload fragments to penetrate to core during the timescale of a thermal quench (TQ)	Higher velocity should permit core penetration before TQ is over
TQ relies on an outside-inside process	Improves probability of inside-out TQ due to deeper core penetration.
Edge deposition requires the need for injecting more radiative material than required for the TQ	Higher assimilation fraction due to core deposition should permit much less payload material injection, providing more capability over controlling $T_e$ in the core to avoid runaway current generation
Injects frozen Ne, Ar, D <sub>2</sub> or combinations of these gases	First generation EPI would inject B, C, BN, W, other solid materials or combinations of these, including a Shell Pellet.
Being tested on multiple tokamaks	Tokamak injection data needed to study and develop EPI payload requirements for ITER and tokamak-based reactors

The capacitor-based power supply is triggered using an ignitron switch that uses liquid mercury as the conducting medium which is more robust to damage from high voltage spikes. An ignitron is better suited for disruption mitigation

application which requires high reliability. Solid state switches such as SCRs would require more attention to switch protection as described in [19, 20]. References [20, 21] describe parallel developments in the application of Rail Guns for disruption mitigation applications.

Control and interlock signals for the EPI are provided by a standalone National Instruments compact RIO controller which utilizes a simple ethernet interface to allow remote operation and easy integration into the host tokamak system.

#### IV. CONCLUSION

Disruption mitigation is the final line of defense for protecting the expensive tokamak infrastructure. Because tokamaks rely on a large amount of plasma current to generate the plasma equilibrium, they have the potential for unavoidable major plasma disruptions. Methods to rapidly quench the discharge after an impending disruption is detected are essential to protect the vessel and internal components of next generation tokamaks and subsequent reactors based on the tokamak concept. The warning time for the onset of some disruptions in tokamaks could be less than 10 ms, which poses stringent requirements on the disruption mitigation system for reactor systems.

The EPI method to inject high velocity granules of the required size for tokamak discharge termination holds great promise for addressing a critical ITER need. The EPI system accelerates a metallic sabot to high velocity by an electromagnetic impeller. At the end of its acceleration, within 2-3 ms, the sabot will release granules of a known velocity and distribution, or a shell pellet containing smaller pellets. The system is fully electromagnetic, with no mechanical moving parts such as pistons or valves, which ensures high reliability after a period of long standby. Table 1 summarizes the major differences between the SPI system currently planned for ITER and the capabilities of the EPI system.

As summarized in the table, a major advantage of the EPI system is that the particles' size, shape and velocity are known. This eases the MHD modeling as it removes a major source of uncertainty and permits more reliable modeling of the entire disruption process. This is particularly important for extrapolating a DMS concept to reactor level systems as present tokamak plasmas are an order of magnitude (or more) smaller in size and energy than those of ITER.

#### REFERENCES

[1] J.E. Menard et al., Prospects for pilot plans based on the tokamak, spherical tokamak and stellarator, *Nucl. Fusion* **51** (2011) 103014

[2] R.S. Granetz, et al., Disruption mitigation studies on ALCATOR C-MOD and DIII-D, *Nuclear Fusion* **47**, 1086 (2007)

[3] N. Commaux, L.R. Baylor, T.C. Jernigan et al., Demonstration of rapid shutdown using large shattered deuterium pellet injection in DIII-D, *Nucl. Fusion* **50**, 112001, (2010).

[4] N.W. Eidiets et al., Poloidal radiation asymmetries during disruption mitigation by massive gas injection on the DIII-D tokamak, *Phys. Plasmas*, **24**, 102504, (2017)

[5] T.C. Luce 2021 Progress on the ITER DMS design and integration 28th IAEA Fusion Energy Conf. (10-15 May) (Virtual Event) p TECH/1-134 ([https://nucleus.iaea.org/sites/fusionportal/Shared%20Documents/FEC%202020/FEC2020\\_ConfMat\\_Online.pdf](https://nucleus.iaea.org/sites/fusionportal/Shared%20Documents/FEC%202020/FEC2020_ConfMat_Online.pdf))

[6] D. Hu, et al., Collisional-radiative simulation of impurity assimilation, radiative collapse and MHD dynamics after ITER shattered pellet injection, *Nucl. Fusion* **63** (2023) 066008

[7] A. Matusyama, et al., Transport simulations of pre-thermal quench shattered pellet injection in ITER: code verification and assessment of key trends, *Plasma Phys. Control. Fusion* **64** (2022) 105018

[8] M. Lehn 2017 ITER Disruption Mitigation Workshop Report (ITER HQ)

[9] T.E. Gebhart, L.R. Baylor and S.J. Meitner, Experimental pellet shatter thresholds and analysis of shatter tube ejecta for disruption mitigation cryogenic pellets, (2020) *IEEE Trans. Plasma Sci.* **48** 1598. <https://doi.org/10.1109/TPS.2019.2957968>

[10] R. Raman, R. Sweeney, R.A. Moyer, et al., Shattered pellet penetration in low and high energy plasmas on DIII-D, *Nuclear Fusion* **60** (2020) 036014. <https://doi.org/10.1088/1741-4326/ab686f>

[11] J. McClenaghan, B.C. Lyons, C.C. Kim, et al., MHD modeling of shattered pellet injection in JET, *Nuclear Fusion* **63** (2023) 066029. <https://doi.org/10.1088/1741-4326/accbd3>

---

[12] D. Hu, E. Nardon, M. Holezl, et al., Radiation asymmetry and MHD destabilization during the thermal quench after impurity shattered pellet injection, *Nuclear Fusion* **61** (2021) 026015. <https://iopscience.iop.org/article/10.1088/1741-4326/abcbc>

[13] V. Leonov et al., Simulation of the pre-thermal quench stage of disruptions during massive gas injection and projections for ITER, *Proceedings of the IAEA-FEC 2014 Conference*, TH/P3-35, St. Petersburg, Russia, October 13-18 October (2014).

[14] R. Raman, R. Lunsford, C.F. Clauser, et al., Prototype tests of the electromagnetic particle injector-2 for fast time response disruption mitigation in tokamaks, *Nuclear Fusion* **61** (2021) 126034 <https://doi.org/10.1088/1741-4326/ac30ca>

[15] R. Lunsford, R. Raman, A. Brooks et al., Modeling of ablant deposition from electromagnetically driven radiative pellets for disruption mitigation studies, *Fusion Science and Technology* (July, 2019).

DOI:10.1080/15361055.2019.1629246.  
<https://www.tandfonline.com/doi/full/10.1080/15361055.2019.1629246>

[16] R. Raman, W.-S. Lay, T.R. Jarboe et al., Electromagnetic particle injector for fast time response disruption mitigation in tokamaks, *Nucl. Fusion* **59** (2019) 016021 (10pp) <https://doi.org/10.1088/1741-4326/aaf192>

[17] E.M. Hollman, et al., Demonstration of tokamak discharge shutdown with shell pellet payload impurity dispersal, *Phys. Rev. Lett.* **122** (2019) 065001

[18] C.T. Holcomb, T.R. Jarboe, A.T. Mattick, D.N. Hill, H.S. McLean et al., Nonperturbing field profile measurements of a sustained spheromak, (2001) *Rev. Sci. Instrum.* **72** 1054. <https://doi.org/10.1063/1.1321741>

[19] E. Spahn et al., 50 kJ ultra-compact pulsed power supply unit for various applications, <https://ieeexplore.ieee.org/document/1665936>

[20] Y.I. Yu et al., Design of an arc suppression system for the electromagnetic pellet injection system, *Fusion Engin. Design* **198** (2024) 114100.

[21] F. Li et al., Development of electromagnetic pellet injector for disruption mitigation of tokamak plasma, *Chinese Phys. B* **32** (2023) 075205